FUEL TEMPERATURE INFLUENCE ON THE PERFORMANCE OF A LAST GENERATION COMMON-RAIL DIESEL BALLISTIC INJECTOR.

PART I: EXPERIMENTAL MASS FLOW RATE MEASUREMENTS AND DISCUSSION

Salvador, F.J., Gimeno, J., Carreres, M. (*), Crialesi-Esposito, M.

CMT-Motores Térmicos, Universitat Politècnica de València

Camino de Vera s/n, E-46022 Spain.

(*) Corresponding author:

Mr. Marcos Carreres, marcarta@mot.upv.es

CMT-Motores Térmicos, Universitat Politècnica de València

Camino de Vera s/n, E-46022 Spain.

Telephone: +34-963876540

FAX: +34-963877659

Salvador, F.J., Gimeno, J., Carreres, M., Crialesi-Esposito, M., "Fuel temperature influence on the performance of a last generation common-rail diesel ballistic injector. Part I: Experimental mass flow rate measurements and discussion".

Energy Conversion and Management 114 (2016), pp. 364-375 (author version)

ABSTRACT

An experimental study is conducted in this paper in order to assess the influence of the fuel temperature on the performance of a last generation common-rail ballistic solenoid injector. Mass flow rate measurements are performed for a wide range of temperatures, extending from 253 to 373 K, representative of all the possible operating conditions of the injector in a real diesel engine, including cold start. The high pressure line and the injector holder were refrigerated, making it possible to carefully control the fuel temperature, whereas measurements at cold conditions were carried out with the help of a climatic chamber. Relevant features such as stationary mass flow, injection delay or the behaviour at the opening and closing stages are analysed together with parameters governing the flow, such as the injector discharge coefficient.

Results show an important influence of the fuel temperature, especially at low injection pressure. A low injection temperature results in a lower stationary mass flow rate, whereas injection duration is also reduced. These results will be explained mainly through the fuel properties variation induced by temperature, together with the ballistic nature of the injector used for the study.

A second part of the paper introduces a one-dimensional model that makes it possible to reproduce these results and further explain them through the analysis of other relevant variables, such as the needle lift.

KEYWORDS

diesel, injection, experimental, fuel temperature, low temperature

LIST OF NOTATION

A_{eff} orifice outlet effective area

A_o orifice outlet area

C_a area coefficient

C_d discharge coefficient

C_v velocity coefficient

c_f fuel speed of sound

Di orifice inlet diameter

D_o orifice outlet diameter

k-factor orifice conicity factor

L orifice length

$\dot{m}$ fuel mass flow

$\dot{m}_{th}$ theoretical fuel mass flow

P pressure

P_0 reference pressure

P_i injection pressure

P_t pressure measured in the IRDCI

Re Reynolds number

r orifice inlet rounding radius

T_i fuel temperature at the injector inlet

t_d delay between SOE and SOI

Salvador, F.J., Gimeno, J., Carreres, M., Crialesi-Esposito, M., "Fuel temperature influence on the performance of a last generation common-rail diesel ballistic injector. Part I: Experimental mass flow rate measurements and discussion".

Energy Conversion and Management 114 (2016), pp. 364-375 (author version)

t_{inj} injection time

u_{eff} effective velocity

u_{th} theoretical velocity

GREEK SYMBOLS:

ΔP pressure drop

μ_f fuel absolute viscosity

ν_f fuel kinematic viscosity: $\nu_f = \frac{\mu_f}{\rho_f}$

ρ_f fuel density

ABBREVIATIONS:

ET Energizing Time

FAME Fatty Acid Methyl Ester

FT-IR Fourier-Transformed Infrared Spectrometry

IRDCI Injection Rate Discharge Curve Indicator

SOE Start of Energizing

SOI Start of Injection

1. INTRODUCTION

The importance of the direct injection system in the diesel engine has attracted the interest of

Salvador, F.J., Gimeno, J., Carreres, M., Crialesi-Esposito, M., "Fuel temperature influence on the performance of a last generation common-rail diesel ballistic injector. Part I: Experimental mass flow rate measurements and discussion".

Energy Conversion and Management 114 (2016), pp. 364-375 (author version)

researchers in the field. Being responsible for the fuel delivery, its role on the ultimate outcome of the engine has been demonstrated in several works: its influence on the quality of the air-fuel mixture has been largely proved [1][2][3], thus highly impacting the combustion phenomenon, fuel consumption and emissions [3][4][5][6][7], key features in the global cleanliness demanded to modern power plants.

Even though many studies, both experimental and computational, have focused on how the diesel injection process and spray development are influenced by factors as the nozzle geometry [8][9][10][11][12][13][14], discharge ambient conditions simulating those of the combustion chamber [15][16][17][18] or fuel injection pressure [19][20], not much attention has been paid to the influence of the fuel temperature itself. However, its effects are deemed to be important, especially when dealing with cold start problems [21][22][23], which are being gradually introduced in the new standards and regulations [24]. Needless to say, the fuel temperature strongly affects the fuel properties, as the authors have reported both at atmospheric and high pressures [25], which in turn play a key role on the injection process. Indeed, Seykens et al. [26] tried to assess the influence of fluid properties on the fuel injection behaviour by means of a one-dimensional computational model. From the experimental point of view, Dernotte et al. [27] or Payri et al. [21][28] analysed the influence of the fuel properties on the spray macroscopic features, also paying attention at the discharge capabilities of the nozzle in the latter case, but left the injector dynamics (transient opening and closing stages) out of the study.

A few works have tried to directly assess the influence of the fuel temperature on the nozzle internal flow and spray formation of diesel direct injection engines. However, most authors focus on a certain range of temperatures. Hence, Tinprabath et al. [24] studied the fuel temperature influence for several biodiesel and diesel blends, focusing on cold temperatures, whereas Park et al. [29] performed a combined numerical and experimental study paying attention to the spray characteristics for relatively warm temperatures only. Finally, Wang et al. [30] studied the cases of 255 and 298 K also paying attention to the influence of fuel temperature on cavitation, but again leaving the injector dynamics out of their scope. It is important to note that nozzle transients, however, have a strong impact on the injection process and spray development as several authors have reported [31][32][33].

In this study, an experimental work on the influence of the fuel temperature on the performance of a Bosch CRI 2.20 injector is conducted. Mass flow rate measurements were performed for a wide range of temperatures (from 253 to 373 K), thus representing all the possible operating conditions of the injector in a real diesel engine, including cold start and the usual situations where the injector is heated by the proximity of the cylinder head. The measurements at cold conditions were carried out with the help of a climatic chamber, and the temperature was carefully controlled through refrigeration. The injector is a solenoid-driven unit [34] of ballistic nature, which means that the needle lift is not mechanically limited to a value that is usually achieved during the normal operation of the injector. Thus, the influence of the fuel properties (which, as it has been said, are strongly affected by the fuel temperature) on the dynamic behaviour of the injector is here deemed to be of even more crucial importance, since the maximum lift reached by the needle will directly depend on its friction with the fuel due to viscous effects. The importance of the fuel temperature is here investigated in terms of stationary mass flow rate, total mass injected, injection delay (time difference between the SOE – start of energizing – and SOI – start of injection), opening and closing slopes or injector discharge coefficient, with the objective of determining in which circumstances these effects should not be neglected due to their subsequent importance in the combustion phenomenon.

As far as the structure of the paper is concerned, it has been divided in 5 sections. First of all, in section 2, a description of the theoretical foundation on which the internal flow features are based is presented. Following, in section 3, the experimental setup is thoroughly described, with special attention to the temperature control. Details on the used fuel and the test matrix analysed are also given in this section. In section 4, results of mass flow rate for all the tested conditions are shown and discussed. From the mass flow rate curves, attention will be paid to the stationary mass flow, total mass injected, injection delay, opening slope, injection duration and injector discharge coefficient (derived from the stationary mass flow values). Finally, the main conclusions of the investigation are drawn in section 5.

In a second part of the paper, a computational one-dimensional model is developed and validated against the experimental results hereby presented. In addition to making it possible to extend the results for any engine operating condition, this model makes it possible to analyse the findings of the present paper in light of internal variables of the injector, such as the needle lift, thus making it possible to acquire a deeper understanding of the phenomena involved.

2. THEORETICAL FOUNDATION

As it has been said, the study is focused on the analysis of mass flow rate measurements at different temperatures. In order to understand how fuel temperature influences the results, it is necessary to introduce the discharge coefficient (C_d) of an orifice, defined as the ratio among the real mass flow rate through the orifice and the theoretical one, as stated in Eq. (1):

$$C_d = \frac{\dot{m}}{\dot{m}_{th}} \qquad (1)$$

The theoretical mass flow rate comes from the mass conservation equation (Eq. (2)):

$$\dot{m}_{th} = \rho_f\, A_o\, u_{th} \qquad (2)$$

where ρ_f is the fuel density, A_0 is the cross-sectional area of the orifice outlet and u_{th} is the theoretical velocity through the orifice, which can be derived from Bernoulli's equation assuming negligible upstream velocity, resulting in the definition of Eq. (3):

$$u_{th} = \sqrt{\frac{2\Delta P}{\rho_f}} \qquad (3)$$

where ΔP is the pressure drop at the orifice. With all, Eq. (1) can be rewritten to express the mass flow rate through an orifice as:

$$\dot{m} = C_d A_o \sqrt{2\rho_f \Delta P} \qquad (4)$$

A direct relation of the fuel temperature to the mass flow rate can already be noticed in Eq. (4) through the fuel density.

Focusing on the discharge coefficient, it can also be broken down into two separate coefficients. These coefficients, defined in Eqs. (5) and (6) relate the effective flow area and velocity (those that lead to the actual mass flow rate through the orifice) to the theoretical ones:

$$C_a = \frac{A_{eff}}{A_o} \qquad (5)$$

$$C_v = \frac{u_{eff}}{u_{th}} \qquad (6)$$

Therefore, the discharge coefficient can also be expressed as:

$$C_d = \frac{\dot{m}}{\dot{m}_{th}} = \frac{\rho_f}{\rho_f}\frac{A_{eff}}{A_o}\frac{u_{eff}}{u_{th}} \qquad (7)$$

Thus, the losses through an orifice can be attributed to an effective loss in area or an effective loss in velocity. In the case of the area coefficient, it can be diminished by a non-uniform velocity profile at the outlet, cavitation or flow separation [35]. With regard to cavitation, a feature that determines the proneness to cavitate of an orifice is its conicity [12], which can be quantified through the *k-factor*:

$$k - factor = \frac{D_i - D_o}{10\ [\mu m]} \qquad (8)$$

where D_i and D_o are the inlet and outlet diameters of the orifice, respectively.

The nozzle of the injector studied in this work is highly conical (as shown in Table 1, where details of the nozzle geometry are given), which means that it is not prone to cavitate. In fact, it will be proven that the nozzle does not cavitate for any of its operating conditions. Hence, the flow regime (laminar, turbulent or transitioning) will be the most influencing factor on the discharge coefficient of this particular nozzle, and can be described by means of the theoretical Reynolds number:

$$Re = \frac{\rho_f\, u_{th}\, D_o}{\mu_f} = \frac{u_{th} D_o}{\nu_f} \qquad (9)$$

where μ_f is the absolute viscosity of the fuel and, alternatively, ν_f is its kinematic viscosity. In fact, it has been found that the discharge coefficient grows asymptotically with the Reynolds number towards a maximum discharge coefficient [36][37]. Thus, it takes low values for laminar flow (low *Re*) where there exists a thicker boundary layer that reduces the effective area and also the effective velocity due to viscous friction [35], whereas after the regime transition it takes high values for turbulent flow (high *Re*), where the velocity profile is more uniform and the viscous friction is reduced. Therefore, this is another mechanism in which the temperature plays an important role due to its influence on *Re* and the flow regime through the fuel density and viscosity.

With all, these flow features are expected to influence the mass flow rate, both in the stationary part of the injection event and in its transient stages, where the needle may partially block the nozzle orifices, reducing their actual effective area and leading to low Re and discharge coefficient values. Also, the importance of the temperature on these features through the fuel properties has been highlighted in this Section in order to make it easier to discuss the results later on.

3. EXPERIMENTAL

3.1 Setup

In the present study, the influence of the fuel temperature on the injection event is assessed through experimental mass flow rate measurements. These measurements were carried out with a commercial IRDCI (Injection Rate Discharge Curve Indicator) from IAV. The working principle of this device is based on the Bosch long tube method [38], which consists on directly injecting into a tube filled with fuel. The injection event produces a pressure increase in the fuel-filled tube that is measured by a piezoelectric pressure sensor and recorded on a data acquisition system. This pressure wave is transmitted along the tube at a certain velocity (c_f, the fuel speed of sound). Considering that the tube has a certain cross-sectional area A_t, the continuity equation leads to the instantaneous mass flow rate through the tube being given by the following expression:

$$\dot{m} = \frac{A_t}{c_f}(P_t - P_0) \qquad (10)$$

where P_t is the pressure measured in the tube and P_0 is a reference pressure. The fuel speed of sound and its variation with pressure and temperature was already determined by the authors as stated in [25] and was taken into account accordingly in this study. A correction for the cumulative phenomenon noticed in the mass flow rate signal was also performed as established in [39]. A scale was placed downstream the IRDCI in order to cross-check the total mass injected per injection event by comparing it to the definite integral of the instantaneous mass flow rate curve.

Fig. 1 shows a scheme of the experimental setup in which the IRDCI was introduced in order to perform the measurements with an appropriate temperature control in the range from 253 to 373 K. Some of the elements that comprised the experimental setup are shown in Fig. 2. A fuel high pressure pump driven by an electric motor extracted and pressurized the fuel contained in a tank after being filtered. As part of a standard procedure, water was recirculated around the fuel to cool it down after the heating suffered due to pressurization in the high pressure pump. It is important to note that water was only recirculated when it was needed to maintain a relatively low temperature, but not when the climatic chamber was in use. After this heat exchange, the fuel travelled through a high pressure flexible line, around which a coolant (glycol) at a proper temperature was also recirculated before the fuel enters the common-rail. The rail was connected to the injector through a 300 mm long high pressure rigid line, which was also cooled or heated by glycol. The fuel inlet temperature and pressure conditions of the tests (hereinafter referred to as T_i and P_i, respectively) were measured in this high pressure rigid line, right upstream the injector (30 mm away from its inlet), where a thermocouple and a pressure sensor were located (see Figs. 1 and 2). The injector was connected to the IRDCI device through an in-built intermediate piece. This piece falls 52 mm upstream the nozzle tip and also made it possible to refrigerate the injector holder, since it has a glycol inlet and an outlet. An extra thermocouple was introduced at this location in order to measure the glycol temperature (see Fig. 1). The glycol came from a heat exchanger where it was heated by an electrical resistance if the fuel temperature needed to be increased. PIDs were used as regulators, acting on the fuel pump (for the pressure) and the glycol heat exchanger (for the temperature). Both the fuel and glycol tanks, the glycol heat exchanger and most of the high pressure flexible line were placed in a climatic chamber (where temperatures down to 248 K can be achieved) with optical access for the coldest temperatures tested (253 and 278 K). The high pressure pump and the IRDCI were kept out of the climatic chamber since otherwise they would have been operating out of their acceptable temperature range. In those conditions, the water cooling system was shut down and all the components upstream the IRDCI are covered by an insulating material that prevented heat exchange with the surroundings. With this setup, in the least favourable case (253 K) it was possible to keep a controlled value of fuel temperature at the inlet (T_i), with differences among this temperature and the glycol temperature at the injector holder lower than 2 K, ensuring virtually uniform and stable temperature conditions in the injector. The IRDCI makes it possible to regulate the fuel backpressure with nitrogen, setting the value with the help of a valve downstream a nitrogen bottle. Fuel from the injector return line was brought back to the fuel tank, whereas the fuel effectively injected in the IRDCI is discharged in a scale, so that the total mass injected per stroke could be recorded and compared to the integral of the mass flow rate curve, as it has already been stated.

3.2 Signal treatment

The injector was driven by a Genotec impulse generator (omitted in Fig. 1), replacing the engine Electronic Control Unit. An injection frequency of 10 Hz was chosen so that a particular injection event was prevented from being influenced by the previous one. Once a tested condition was achieved, the injection was run by at least 100 seconds before recording the measurements, giving a minimum of 1000 warm-up injections so that stable conditions were attained. The pressure signal from the IRDCI piezoelectric sensor was amplified, visualized in an oscilloscope and recorded in a computer together with the pressure signal in the high pressure line and the corresponding temperature values. 50 injections per operating point were recorded, averaging both the mass flow rate and pressure signal curves. A second set of 50 injections was also measured to ensure no dispersion nor anomalous data in the results.

An example of an averaged mass flow rate curve together with its corresponding energizing signal is shown in Fig. 3. The criteria to extract information from the curve are shown in the figure. The SOI was determined by calculating the opening slope where the mass flow was among the 10% and the 50% of the maximum achieved and intersecting the resulting curve with the value of null mass flow rate. This gives the injection delay (time difference among SOE and SOI), t_d, as shown. The time of injector closing was determined in an analogous way, leading to the injection time, t_{inj}. The stationary stage was established as the stage on which the mass flow rate was above 95% of its maximum value. The average of the mass flow rate in the stationary stage was computed for the longest points tested, making it possible to calculate the injector discharge coefficient as shown in Eq. (11) (recall Eqs. (1) to (4)):

$$C_d = \frac{\dot{m}}{A_o\sqrt{2\rho_f(P_i - P_b)}} \qquad (11)$$

where P_i is the nominal injection pressure and P_b the nominal backpressure. The area A_o is determined from the number of nozzle orifices and the orifices outlet diameter D_o (recall Table 1).

3.3 Test Matrix

The conditions tested in the study are listed in Table 2. They were chosen in order to cover most engine-like operating conditions, including from cold start to a long engine run, both low, intermediate and high typical pressure values and both short and long injections. The longest energizing times of 2 ms ensure a long period of stabilized mass flow rate so that the injector discharge coefficient could be accurately determined. All the combinations among variables were tested, thus leading to a total of 80 operating points.

3.4 Fuel

A standard winter fuel was chosen for the study in order to ensure proper operation at low temperatures. The values of density and viscosity (both absolute and kinematic) at atmospheric pressure and the different temperatures tested are listed in Table 3, and shown in Fig. 4 for illustrative purposes due to their importance when interpreting the results. The density was measured with a standard hydrometer as established by the ASTMD1298, with an estimated accuracy of ±5 x 10-4 kg/m^3, whereas the viscosity was measured with a commercial capillary viscometer following the ASTM D-445 standards. Table 3 also shows the water content, determined in accordance to the ISO 12937. In addition, the fatty acid methyl esters (FAME) volume percentage was quantified based on the ASTM D7806-12 standard, using Fourier-Transformed Infrared Spectrometry (FT-IR). First, a calibration curve was obtained with known concentrations of FAME in pure conventional fuel. After that, samples of the fuel tested in this work were compared to that calibration curve. The viscosity values at 253 K were extrapolated.

Additionally, the density and speed of sound of the fuel at different temperatures and pressures were determined in [25]. In that study, the authors established correlations for those properties. Thus, their values at the temperature and pressure levels tested in the present study have been easily obtained from those correlations as shown in Fig. 5. It can be seen that both variables decrease with temperature and increase with pressure. In the case of the speed of sound, its evolution with the temperature is linear, whereas the influence of the pressure is slightly more important at high temperatures. On the other hand, the density decrease with the temperature is not totally linear, the influence of the pressure also being more important at high temperatures. These trends will be useful to discuss the results presented in Section 4.

4. RESULTS AND DISCUSSION

4.1 Mass flow rate curves

The experimentally determined mass flow rate curves for all the tested conditions are shown in Fig. 6. Each plot represents an injection pressure, for which all tested temperatures are depicted. The temperature case of 353 K has been omitted in this figure due to the similarities with the 373 K case.

The effect of temperature can be appreciated in the figure. Influence on the opening slope and injection delay will be analysed in following subsections, but it can already be seen that it seems more relevant at low injection pressures. Similarly, the stationary mass flow rate is more affected by the temperature at low injection pressures. This fact is also analysed in Section 4.2. Anyway, the most important effect of the fuel temperature that can be appreciated is the injection duration. It can be seen that it is noticeably reduced at low temperatures. This can be explained due to the ballistic nature of the injector. As it was shown in Fig. 4, the fuel absolute viscosity decreases with the fuel temperature. This results in a lower friction of the needle against the fuel during the injector opening stage, which leads to higher maximum needle lifts achieved the higher the fuel temperature is. Thus, during the closing stage, the needle falls from a higher position when the fuel temperature is increased. Since the effect of the fuel temperature on the closing slope seems negligible, this fact leads to a higher time for the needle to close against its seat and cut the injection. It is also important to mention that the effect of the fuel temperature on the injection duration seems to be more important at the lowest temperature (253 K), for which the injection duration is reduced in a much more substantial way as compared to 273 K. Recalling Fig. 4, this is due to the fact that the fuel absolute viscosity grows exponentially when the fuel temperature decreases, whereas the influence of the temperature on viscosity is not as important for higher temperatures.

4.2 Stationary mass flow rate

Information on the values of stationary mass flow rate have been extracted for the points with an ET of 2 ms, as explained in Section 3.2. The values are listed in Table 4 and they have been represented in Fig. 7 both against the square root of the pressure drop for each tested temperature and against the fuel temperature for each tested injection pressure. The stationary mass flow rate increases almost linearly with the square root of the pressure drop, as expected [19]. A first important fact that can be observed is that the nozzle does not seem to be working under cavitation conditions in any case, since a mass flow rate collapse is not noticed. As it was stated in Section 2, this result is expected considering the high degree of convergence of the nozzle orifices.

Focusing on the temperature influence on the stationary mass flow for a given injection pressure, Fig. 7 also reveals that, at low injection pressures, the stationary mass flow rate increases with the fuel temperature, with a difference of about 6% among the extreme cases. However, this trend is not noticed at higher injection pressures, where the differences among temperatures do not seem to be as relevant in percentage terms.

In order to analyse these results, it is important to note that there are two mechanisms with opposed effects through which the fuel temperature is influencing the stationary mass flow, as can be derived recalling Eq. (4). On one hand, a mass flow rate decrease is expected with higher fuel temperatures due to the lower densities induced, also at pressures higher than the atmospheric (recall Fig. 5). On the other hand, the mass flow rate also depends on the discharge coefficient. As explained in Section 2, the discharge coefficient grows asymptotically with the Reynolds number, which in turn depends on the fuel density and viscosity. Considering Eq. (9) and the definition of Re that involves the kinematic viscosity, higher fuel temperatures lead to lower Re (recall Fig. 4), thus leading to lower values of C_d. With all, it is necessary to consider both effects together in order to understand the influence of the fuel temperature on the stationary mass flow.

Fig. 8 shows the evolution of the injector C_d against *Re* for the tested conditions. The discharge coefficient values have been calculated according to Eq. (11). The expected asymptotic growth of C_d with *Re* for non-cavitating orifices is observed. It can be seen that, for high temperatures and high injection pressures, the high *Re* leads to the nozzle orifices working in the turbulent zone, with only slight variations in C_d due to the fact that the velocity profile is nearly uniform and the friction losses along the orifice are minimized, as stated in Section 2. However, the nozzle is working in the laminar-turbulent transition zone for the lowest *Re* values tested, obtained for the lowest injection pressures and temperatures within the injector operating conditions. In this region, the flow velocity profile in the nozzle is not uniform and there is a boundary layer in part of the nozzle orifices length whose thickness directly increases the losses due to friction. This induces a lower effective area for the flow together with a lower effective velocity near the wall, resulting in lower values of both C_a and C_v, which in turn lead to the lower values of C_d appreciated.

In summary, the trends observed in Fig. 7 can be explained in view of the previous reasoning. At low injection pressures the temperature effects on the flow regime lead to high variations in the discharge coefficient, able to overcome the stationary mass flow rate reduction due to the density changes when the temperature increases. When the fuel injection pressure is higher and the flow gets more turbulent, except for the case of T_i = 253 K, the variation of the discharge coefficient with the temperature is not as important and it is not able to invert the trend established by the density effect. In these situations, both conflicting effects of the fuel temperature seem to have the same importance and no particular trend can be established, obtaining virtually the same stationary mass flow for all temperatures (variations among the extreme cases for P_i = 120 MPa are only 1.1%). That is also the reason why the stationary mass flow at T_i = 273 K stops being one of the lowest values at low pressure to be the highest one at high pressure. However, at T_i = 253 K the *Re* values are low even at the highest injection pressure, making the nozzle work in the laminar-turbulent transition. This explains why the highest stationary mass flow rates are not obtained for this temperature (which would be expected by the sole influence of the density), being achieved for 273 K instead, for which the discharge coefficient is not as substantially modified by pressure as the density is.

4.3 Injector dynamics

The dynamics of the injector can also be analysed from the experimental mass flow rate measurements. Fig. 9 shows a detail of the first instants of the mass flow rate curves, in order to analyse the impact of the fuel temperature on the opening stage. It can be observed that the fuel temperature does not importantly affect the opening slope of the mass flow rate curve at any injection pressure. However, it can be seen that it directly affects the injection delay, t_d, that was defined in Section 3.2 and Fig. 3. The evolution of the injection delay (t_d) with the injection pressure for the different injection temperatures tested is shown in Fig. 10. It can be seen that the injection delay is reduced when the injection pressure is increased. This result agrees with those reported by other authors [40] and is expected since the injector opening takes place due to an unbalance of pressure forces above and below the needle. This unbalance will be higher the higher the injection pressure is.

Focusing on a given injection pressure it can be seen that, in general, the injection delay is reduced when the temperature increases. This can be explained due to the fact that another parameter influencing needle dynamics is the fuel viscosity, since it is directly related to the viscous forces that oppose the needle movement. As already discussed in Section 4.1, the viscosity is reduced the higher the temperature is (recall Fig. 4). This influence is more important at low temperatures, for which the viscosity increases exponentially. This is the reason why the differences in injection delay among temperatures are more significant at low pressures, where the needle opening is governed by the friction forces induced by fuel viscosity, as opposed to the higher injection pressures, where needle dynamics is more importantly dominated by the pressure unbalance and the differences in injection delay get gradually reduced.

As it has already been commented in Section 4.1 due to its high visibility in the mass flow rate curves, the injection duration is highly affected by the fuel temperature due to the ballistic nature of the injector and the different values of maximum lift achieved by the needle. Fig. 11 summarizes the results of injection duration t_{inj}, processed as defined in Section 3.2 and Fig. 3. As intuition dictates considering that the injector is ballistic, the injection time increases linearly with the energizing time for a given injection pressure and temperature, since each of those conditions will lead to a different value of maximum needle lift from which the needle will have to fall in order to close against its seat. Nevertheless, the highest injection pressure P_i = 180 MPa shows an exception to this trend when the injector is energized in the range of 1 to 2 ms. This fact could be explained if the injector reaches its maximum lift for those conditions. In those cases, the differences seen from temperature to temperature could be attributed to a different elastic deformation of the needle due to its thermal expansion, since no significant differences in the closing slope have been reported (recall Fig. 6). It is also important to highlight that the most important differences in injection time among temperatures happen at the coldest conditions, from 253 to 273 K. Again, this is due to the fact that the fuel viscosity increases exponentially at the lowest temperatures.

4.4 Total mass injected

The total mass injected for each tested condition has been determined by integrating the corresponding mass flow rate curve and comparing it to the weight measured by the scale, as explained in Section 3. Fig. 12 shows the results for each tested condition. The observed trends are similar to those found for the injection duration and analysed in Section 4.3 and Fig. 11. This fact makes it possible to state that the highest effect through which the fuel temperature influences the injected mass is injection duration, overcoming the effects on injection delay or stationary mass flow rate that have already been discussed along the present Section. Therefore, a reduction in fuel temperature leads to lower mass quantities injected in the cylinder. This influence is more important at sub-zero temperatures due to the high influence on the fuel viscosity. This fact should not be neglected due to its importance during cold start, where it could be desirable for the ECU to act in order to enlarge the energizing times for a given condition so that the quantities of fuel burnt are not resented. As a matter of fact, differences ranging from 70% to 80% have been reported among the extreme temperatures at all pressure and an energizing time of 0.5 ms. These differences are still important at higher energizing times (1 ms) where the mass flow rate remains stabilized for a longer period, ranging from 30% to 40% among the extreme temperatures at all pressures.

5. CONCLUSIONS

The fuel temperature influence on the injection process has been assessed in this paper through experimental mass flow rate measurements. A methodology to carefully control the injection temperature has been successfully applied in order to gather data in a wide range of conditions, from 253 to 373 K. This methodology includes the use of a climatic chamber for the coldest conditions.

The main conclusions of the study are summarized in the following points:

- The stationary mass flow is influenced by the fuel temperature at low injection pressures and temperatures. In low pressure conditions, the flow is in the laminar-turbulent transition due to the low Reynolds number associated. This Reynolds number will get even lower the lower the injection temperature is, due to the important increase in kinematic viscosity. A reduction in the Reynolds number progressively increases the thickness of the existent boundary layer, increasing the losses due to viscous friction and effectively reducing the flow area, leading to low values of discharge coefficient that affect the flow. This leads to differences of about 6% in the extreme cases. Nevertheless, in medium to high pressure conditions, the Reynolds number gets high and the flow becomes fully turbulent, without important variations in the discharge coefficient with the fuel temperature. In these conditions, the effect of the temperature on the fuel density becomes dominant and governs the flow, thus inverting the previous trend and leading to the low temperature of 273K resulting in the highest stationary mass flow rates, with these values gradually decreasing when the fuel temperature increases. The exception is 253 K, for which the Reynolds number is still low enough to lead to low discharge coefficients that affect the flow in a similar manner to the density. The differences among stationary mass flow rates at medium and high pressure, however, are not particularly relevant.

- Injector opening is affected by temperature, especially at low injection pressures. In these conditions, needle dynamics is strongly affected by fuel viscosity, due to the needle-fuel friction. Thus, lower temperatures result in higher viscous forces opposing the needle movement, leading to higher injection delays. This effect is more important at low temperatures, where small reductions in temperature lead to huge increases in viscosity. When the injection pressure is increased, the needle dynamics stops being governed by the viscous effects and the pressure unbalance is more relevant. Thus, even when the trend with the temperature is respected, the variations among temperatures for a given injection pressure are not as important.

- Even though the needle dynamics is affected by the fuel temperature leading to different injection delays, no significant influence has been reported on the slope of the opening stage of the mass flow rate curves.
- Injection duration is the parameter most importantly affected by fuel temperature, being importantly reduced the lower the temperature is. This fact is explained due to the ballistic nature of the injector. Thus, the higher viscous friction associated to the low temperatures results in the needle reaching lower maximum positions, from which it will have to fall when the injector stops being energized. This results in lower distances for the needle to travel in order to close against its seat, thus cutting the injection at earlier times after the energizing.
- With regard to the total mass injected, the trends are similar to the ones seen for the injection duration, since this parameter has been proven to be influenced by fuel temperature in a more important way than the stationary mass flow or the injector opening. This fact needs to be taken into account at cold start, where substantially lower amounts of fuel may be introduced into the cylinder: differences up to 70% among the extreme temperature cases have been found for all pressures at an energizing time of 0.5 ms, still reaching 40% for the 1 ms case. In these conditions, it may be desirable to act on the ECU in order to enlarge the injector energizing times to compensate this phenomenon.

ACKNOWLEDGEMENTS

This work was partly sponsored by “Ministerio de Economía y Competitividad” in the frame of the project “Comprensión de la influencia de combustibles no convencionales en el proceso de inyección y combustión tipo diesel”, reference TRA2012-36932. The equipment used in this work has been partially supported by FEDER project funds "Dotación de infraestructuras científico técnicas para el Centro Integral de Mejora Energética y Medioambiental de Sistemas de Transporte (CiMeT), (FEDER-ICTS-2012-06)", in the frame of the operation program of unique scientific and technical infrastructure of the Ministry of Science and Innovation of Spain. This support is gratefully acknowledged by the authors.

The authors would also like to thank José Enrique del Rey and Santiago Lacruz for their technical help on the experimental setup and their support during the measurements.

REFERENCES

[1] Lefèbvre, A.H., Atomization and Sprays, Hemisphere, 1989, ISBN 0891166033.

[2] Hiroyasu, H., Arai, M., Structures of fuel sprays in Diesel engines, SAE Paper 900475, 1990.

[3] Payri, R., Salvador, F.J., Gimeno, J., De la Morena, J., Influence of injector technology on injection and combustion development – Part 2: Combustion analysis, Applied Energy, 88 (2011), pp. 1130-1139.

[4] Erlach, H., Pressure modulated injection and its effect on combustion and emissions of a HD diesel engine, SAE Paper 952059, 1995.

[5] Park, S.H., Yoon, S.H., Lee, C.S., Effects of multiple-injection strategies on overall spray behavior, combustion, and emissions reduction characteristics of biodiesel fuel, Applied Energy, 88(1) (2011), pp. 88-98.

[6] Som, S., Ramirez, A.I., Longman, D.E., Aggarwal, S.K., Effect of nozzle orifice geometry on spray, combustion, and emission characteristics under diesel engine conditions, Fuel, 90 (2011), pp. 1267-1276.

[7] Agarwal, A.H., Dhar, A., Gupta, J.G., Kim, W.I., et al., Effect of fuel injection pressure and injection timing of Karanja biodiesel blends on fuel spray, engine performance, emissions and combustion characteristics, Energy Conversion and Management, 91 (2015), pp. 302-314.

[8] Sayin, C., Gumus, M., Canakci, M., Influence of injector hole number on the performance and emissions of a DI diesel engine fueled with biodiesel-diesel fuel blends, Applied Thermal Engineering, 61 (2014), pp. 121-128.

[9] von Kuensberg Sarre, C., Kong, S., Reitz, R., Modeling the Effects of Injector Nozzle Geometry on Diesel Sprays", SAE Technical Paper 1999-01-0912, 1999.

[10] Bermúdez, V., Payri, R., Salvador, F.J., Plazas, A., Study of the influence of nozzle seat type on injection rate and spray behaviour, Proceedings of the Institution of Mechanical Engineers, Part D: Journal of Automobile Engineering, 219 (2005), pp. 677-689.

[11] Lee, C.W., Kim, I., Koo, K.W., Park, J., et al., Experimental study of the effects of nozzle hole geometry for a DI diesel engine. Proceedings of ICLASS 2006, Kyoto, Paper ID ICLASS06-203.

[12] Payri, F., Payri, R., Salvador, F.J., Martínez-López, J., A contribution to the understanding of cavitation effects in Diesel injector nozzles through a combined experimental and computational investigation, Computer and Fluids, 33 (2009), pp. 941-947.

[13] Salvador, F.J., Martínez-López, J., Caballer, M., De Alfonso, C., Study of the influence of needle lift on the internal flow and cavitation phenomenon in diesel injector nozzles by CFD using RANS methods, Energy Conversion and Management, 66 (2013), pp. 246-256.

[14] Sun, Z.Y., Li, X., Chen, C., Yu, Y., et al., Numerical investigation on effects of nozzle's geometry parameters on the flow and the cavitation characteristics within injector's nozzle for a pressure common-rail DI diesel engine, Energy Conversion and Management, 89(1) (2015), pp. 843-861.

[15] Naber, J., Siebers, D., Effects of Gas Density and Vaporization on Penetration and Dispersion of Diesel Sprays, SAE Technical Paper 960034, 1996.

[16] Roisman, I.V., Araneo, L, Tropea, C., Effect of ambient pressure on penetration of a diesel spray, International Journal of Multiphase Flow, 33(8) (2007), pp. 904-920.

[17] Payri, F., Payri, R., Bardi, M., Carreres, M., Engine combustion network: Influence of the gas properties on the spray penetration and spreading angle, Experimental Thermal and Fluid Science, 53 (2014), pp. 236-243.

[18] Payri, R., Salvador, F.J., Gimeno, J., Soare, V., Determination of diesel sprays characteristics in real engine in-cylinder air density and pressure conditions, Journal of Mechanical Science and Technology, 19(11) (2005), pp. 2040-2052.

[19] Payri, R., Salvador, F.J., Gimeno, J., Novella, R., Flow regime effects on non-cavitating injection nozzles over spray behavior, International Journal of Heat and Fluid Flow, 32(1) (2011), pp. 273-284.

[20] Gumus, M., Sayin, C., Canakci, M., The impact of fuel injection pressure on the exhaust emissions of a direct injection diesel engine fueled with biodiesel-diesel fuel blends, Fuel, 95(1) (2012), pp. 486-494.

[21] Payri, R., Salvador, F.J., Gimeno, J., Bracho, G., Understanding Diesel Injection Characteristics in Winter Conditions, SAE Technical Paper 2009-01-0836, 2009.

[22] Vergnes, C., Foucher, F., Mounaïm, R.C., Discharge coefficient for a diesel injector during cold starting conditions, Atomization and Sprays, 19(7) (2009), pp. 621-631.

[23] Francisco, J., Jiménez, E., Experimental analysis of low temperature combustion mode with diesel and biodiesel fuels: A method for reducing NOx and soot emissions, Fuel Processing Technology, 103 (2012), pp. 57-63.

[24] Tinprabath, P., Hespel, C., Chanchaona, S., Foucher, F., Influence of biodiesel and diesel fuel blends on the injection rate and spray injection under cold conditions, ILASS – Europe 2014, 26th Annual Conference on Liquid Atomization and Spray System, Bremen, 2014

[25] Desantes, J.M., Salvador, F.J., Carreres, M., Jaramillo, D., Experimental Characterization of the Thermodynamic Properties of Diesel Fuels Over a Wide Range of Pressures and Temperatures, SAE International Journal of Fuels and Lubricants, 8(1) (2015), pp. 190-199.

[26] Seykens, X.L.J., Somers, L.M.T., Baert, R.S.G., Modelling of common rail fuel injection system and influence of fluid properties on injection process, Proceedings of VAFSEP, Dublin, 2004.

[27] Dernotte, J., Hespel, C., Houillé, S., Foucher, F., et al., Influence of fuel properties on the diesel injection process in nonvaporizing conditions, Atomization and Sprays, 22(6) (2012), pp. 461-492.

[28] Payri, R., Salvador, F.J., Gimeno, J., Bracho, G., Effect of fuel properties on diesel spray development in extreme cold conditions, Proceedings of the Institution of Mechanical Engineers, Part D: Journal of Automobile Engineering, 222 (2008), pp. 1743-1753.

[29] Park, S.H., Kim, H.J., Suh, H.K., Lee, C.S., Experimental and numerical analysis of spray-atomization characteristics of biodiesel fuel in various fuel and ambient temperature conditions, International Journal of Heat and Fluid Flow, 30 (2009), pp. 960-970.

[30] Wang, Z., Ding, H., Wyszynski, M.L., Tian, J., et al., Experimental study on diesel fuel injection characteristics under cold start conditions with single and split injection strategies, Fuel Processing Technology, 131 (2015), pp. 213-222.

[31] Lee, J., Min, K., Kang, K., Bae, C.S., et al., Effect of piezo-driven and solenoid-driven needle opening of common-rail diesel injectors on internal nozzle flow and spray development, International Journal of Engine Research, 7(6) (2006), pp. 489-502.

[32] Kostas, J., Honnery, D., Soria, J., Kastengren, A., et al., Effect of nozzle transients and compressibility on the penetration of fuel sprays, Applied Physics Letters, 95 (2009).

[33] Pickett, L., Manin, J., Payri, R., Bardi, M., et al., Transient Rate of Injection Effects on Spray Development, SAE Technical Paper 2013-24-0001, 2013.

[34] Zeh, D., Hammer, J., Uhr, C., Rückle, M., et al., Bosch Diesel Injection Technology – Response for Every Vehicle Class, 23rd Aachen Colloquium Automobile and Engine Technology, Aachen, 2014.

[35] Payri, R., Salvador, F.J., Gimeno, J., García, A., Flow regime effects over non-cavitating diesel injection nozzles, Proceedings of the Institution of Mechanical Engineers, Part D: Journal of Automobile Engineering, 226 (2011), pp. 133-144.

[36] Lichtarowicz, A.K., Duggins, R.K., Markland, E., Discharge coefficients for incompressible non-cavitating flow through long orifices, Journal of Mechanical Engineering Science, 7(2) (1965), pp. 210-219.

[37] Schmidt, D.P., Corradini, M.L., The internal flow of diesel fuel injector nozzles: A review, International Journal of Engine Research, 2(1) (2001), pp. 1-22.

[38] Bosch, W., The Fuel Rate Indicator: A New Measuring Instrument For Display of the Characteristics of Individual Injection, SAE Technical Paper 660749, 1966.

[39] Payri, R., Salvador, F.J., Gimeno, J., Bracho, G., A new methodology for correcting the signal cumulative phenomenon on injection rate measurements, Experimental Techniques, 32(1) (2008), pp. 46-49.

[40] Armas, O., Martínez-Martínez, S., Mata, C., Pacheco, C., Alternative method for bulk modulus estimation of Diesel fuels, Fuel, 167 (2016), pp. 199-207.

Table 1: Summary of nozzle geometrical parameters.

Table 2: Experimental mass flow rate measurements test matrix.

Table 3: Fuel properties at atmospheric pressure.

Table 4: Stationary values of mass flow rate for the different tested conditions with ET = 2 ms.

Figure 1: Experimental setup for the mass flow rate measurements. The thermocouple and pressure sensor locations are shown in the diagram.

Figure 2: Actual elements of the experimental setup for the mass flow rate measurements.

Figure 3: Generic mass flow rate curve together with its corresponding energizing signal.

Figure 4: Fuel density and viscosity evolution with the temperature at atmospheric pressure.

Figure 5: Fuel density and speed of sound evolution with the temperature for the different pressures tested.

Figure 6: Mass flow rate curves for all the tested conditions.

Figure 7: Evolution of the stationary mass flow rate with the injection pressure for the different temperatures tested (top) and its evolution with the fuel temperature for the different pressures tested (bottom). Values have been normalized with the square root of ΔP in the latter.

Figure 8: Injector discharge coefficient evolution against Re for the different tested conditions.

Figure 9: Detail of mass flow rate curves to highlight the injector behaviour on the opening stage.

Figure 10: Evolution of the injection delay with the injection pressure for the different temperatures tested.

Figure 11: Injection time for all the tested conditions.

Figure 12: Total mass injected for all the tested conditions.

Property	Value
Number of holes [-]	7
D_i [µm]	146
D_o [µm]	117
k-factor [µm]	2.8
L [µm]	710
r [µm]	27

Table 1: Summary of nozzle geometrical parameters.

Property	Values tested
Fuel injection temperature, Ti [K]	253 - 273 - 303 - 353 - 373
Injection pressure, Pi [MPa]	40 - 70 - 120 - 180
Energizing Time [ms]	0.25 - 0.5 - 1 - 2
Backpressure [MPa]	4

Table 2: Experimental mass flow rate measurements test matrix.

Fuel temperature [K]	Density [kg/m^3]	Absolute viscosity [cP]	Kinematic viscosity [cSt]	Water content [mg/kg]	Fatty acid methyl esters (% volume)
253	851	15.32	18.00		
273	838	5.87	7.00		
303	820	2.71	3.30	31.74	2.30
353	785	1.1	1.40		
373	775	0.85	1.10		

Table 3: Fuel properties at atmospheric pressure.

	Stationary mass flow rate [g/s]			
Temperature [K] / Pressure [MPa]	40	70	120	180
253	14.09	19.79	27.76	34.56
273	14.2	20.31	27.94	35.37
303	14.43	20.49	27.89	34.94
353	14.74	20.69	27.99	34.87
373	14.93	20.58	27.67	34.64

Table 4: Stationary values of mass flow rate for the different tested conditions with ET = 2 ms.

Salvador, F.J., Gimeno, J., Carreres, M., Crialesi-Esposito, M., "Fuel temperature influence on the performance of a last generation common-rail diesel ballistic injector. Part I: Experimental mass flow rate measurements and discussion".

Energy Conversion and Management 114 (2016), pp. 364-375 (author version)

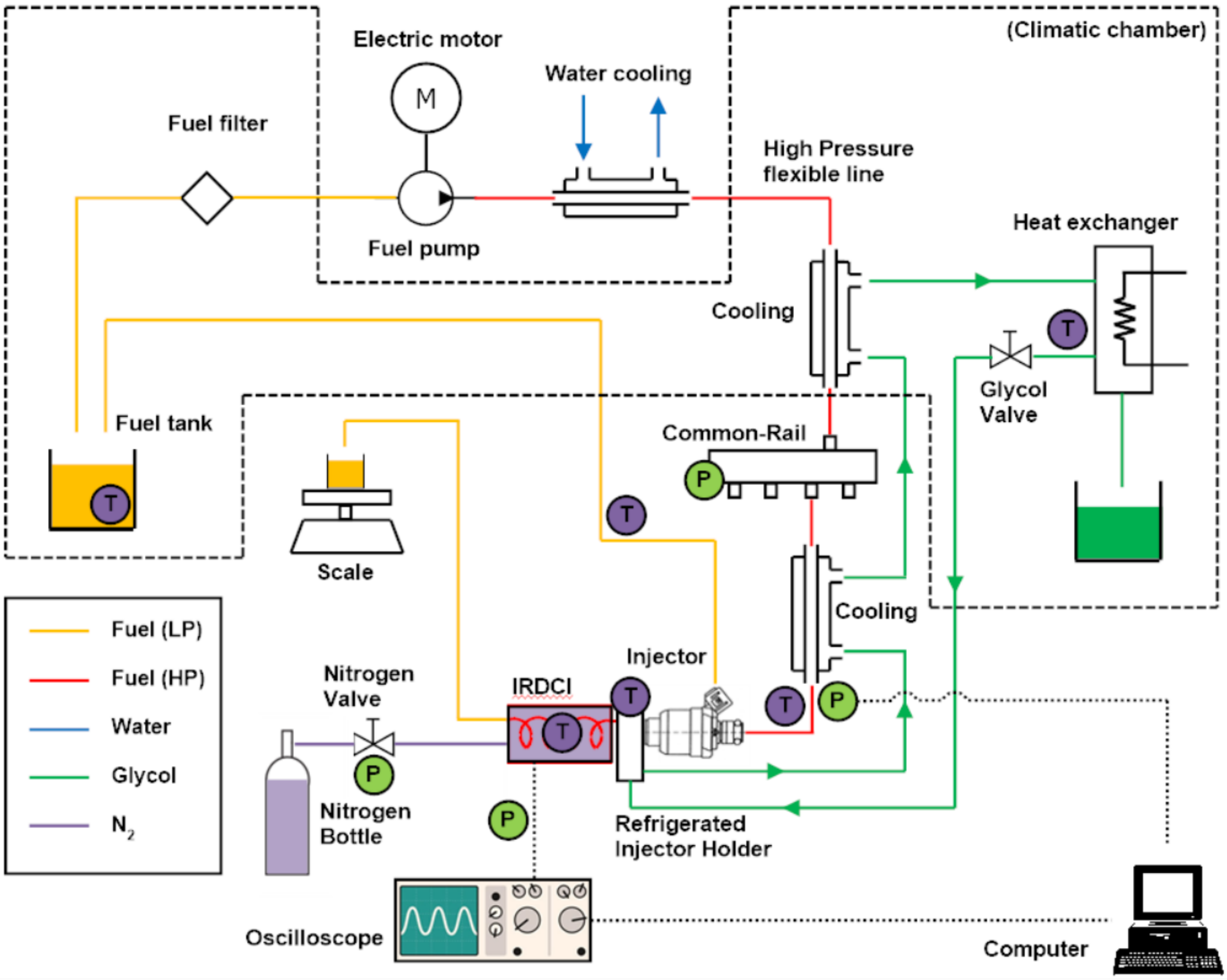

Figure 1: Experimental setup for the mass flow rate measurements. The thermocouple and pressure sensor locations are shown in the diagram.

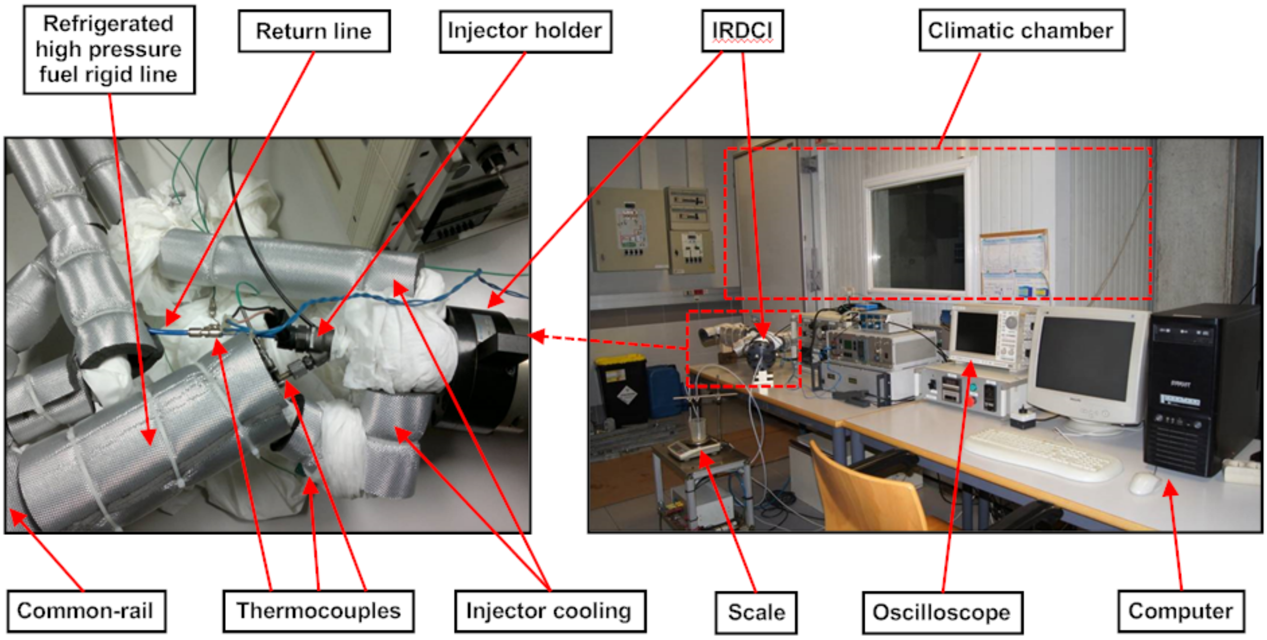

Figure 2: Actual elements of the experimental setup for the mass flow rate measurements.

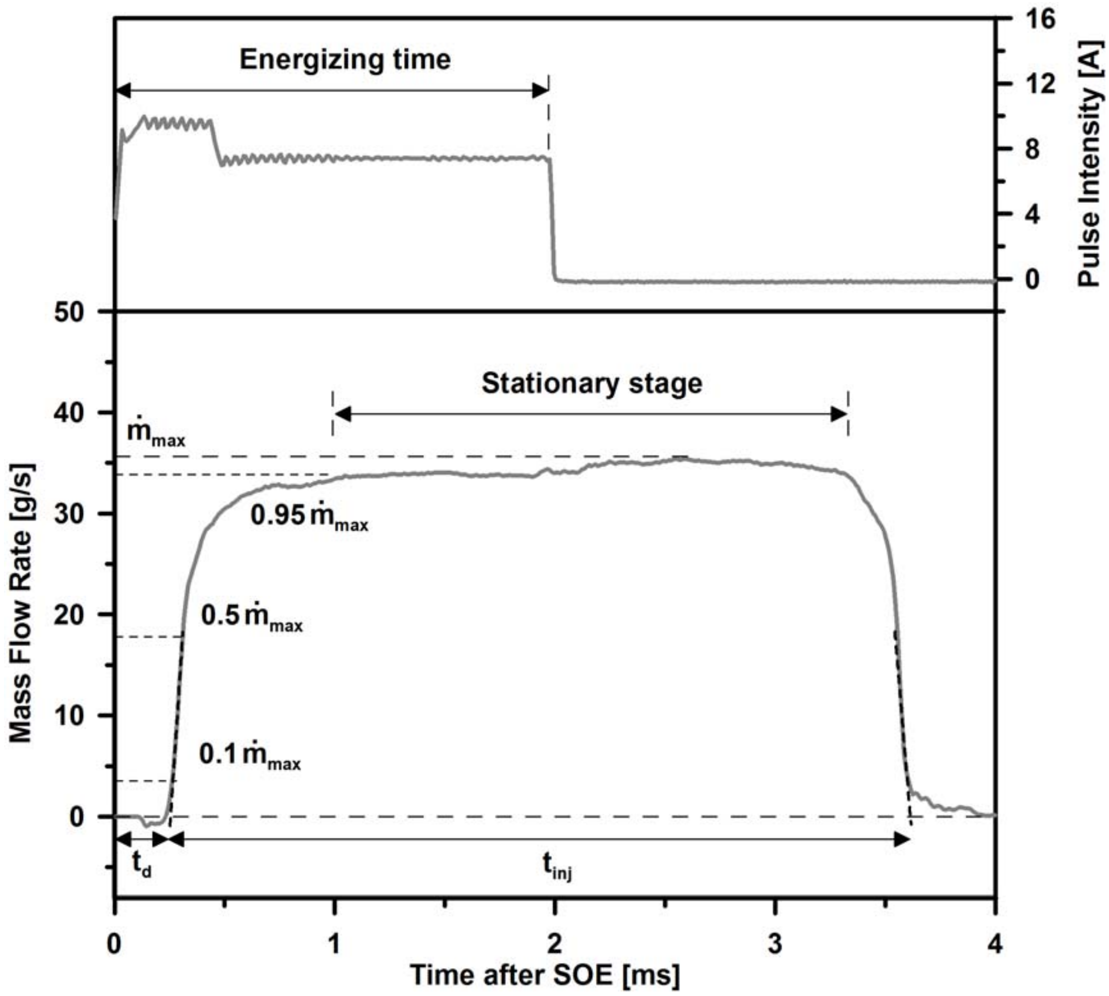

Figure 3: Generic mass flow rate curve together with its corresponding energizing signal.

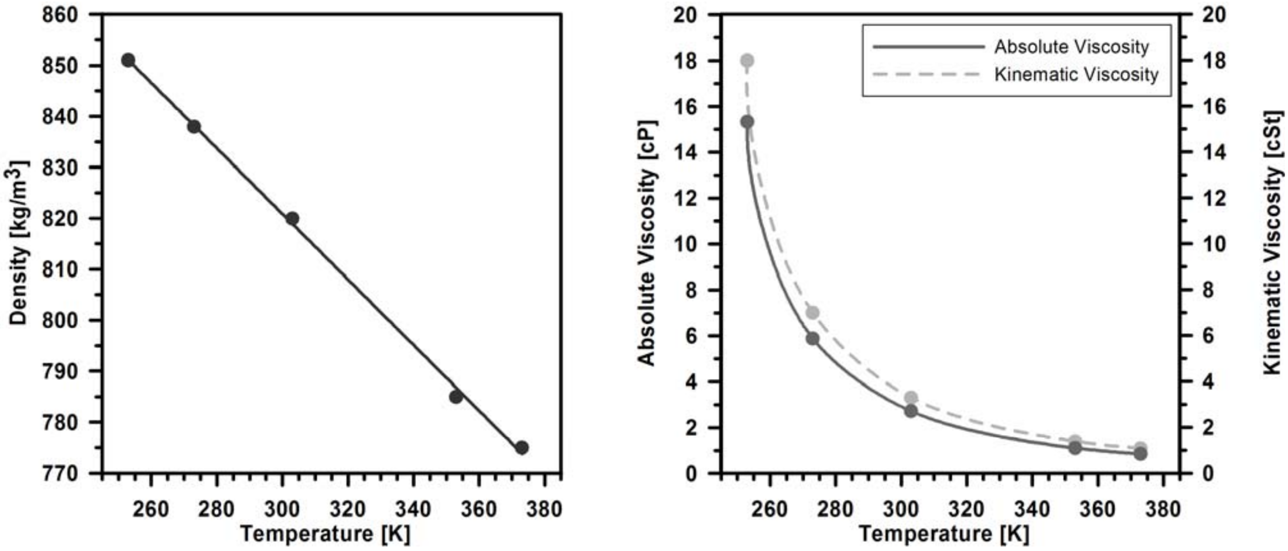

Figure 4: Fuel density and viscosity evolution with the temperature at atmospheric pressure.

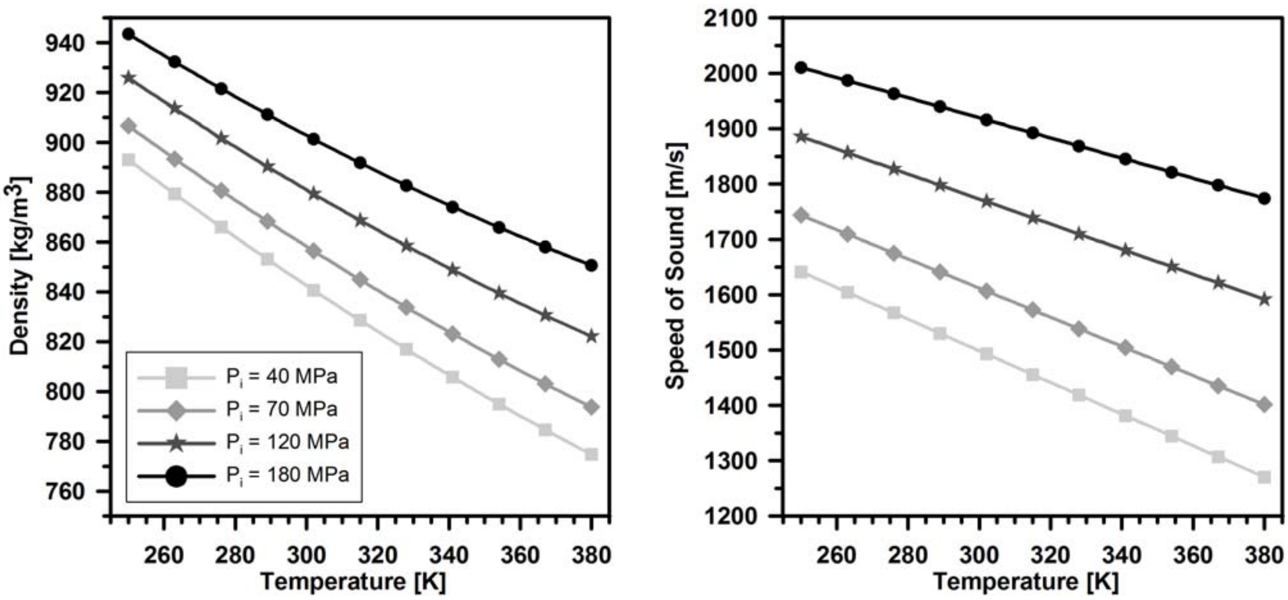

Figure 5: Fuel density and speed of sound evolution with the temperature for the different pressures tested.

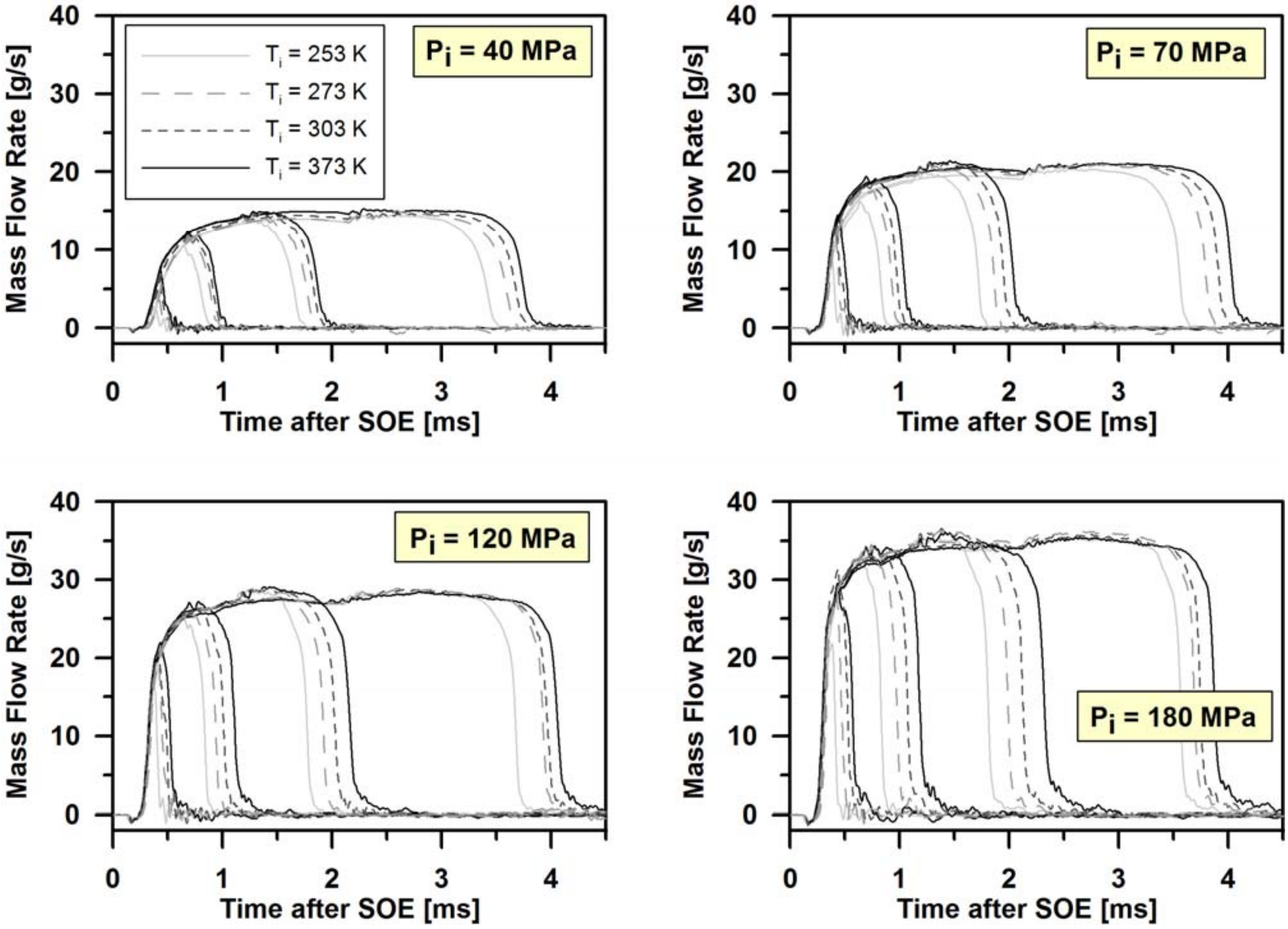

Figure 6: Mass flow rate curves for the tested conditions. Results for T_i = 353 K have been omitted in the figure. All the tested energizing times have been represented.

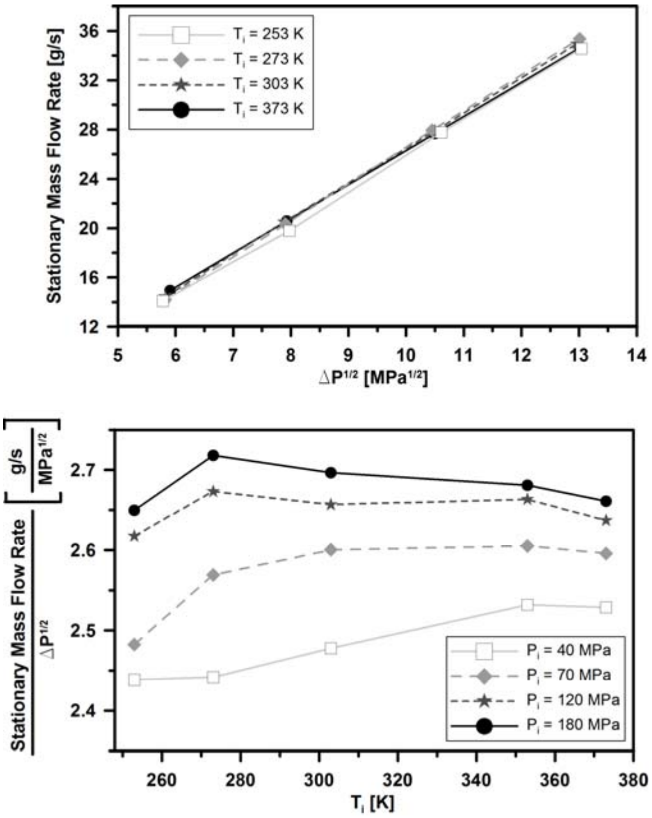

Figure 7: Evolution of the stationary mass flow rate with the injection pressure for the different temperatures tested (top) and its evolution with the fuel temperature for the different pressures tested (bottom). Values have been normalized with the square root of ΔP in the latter.

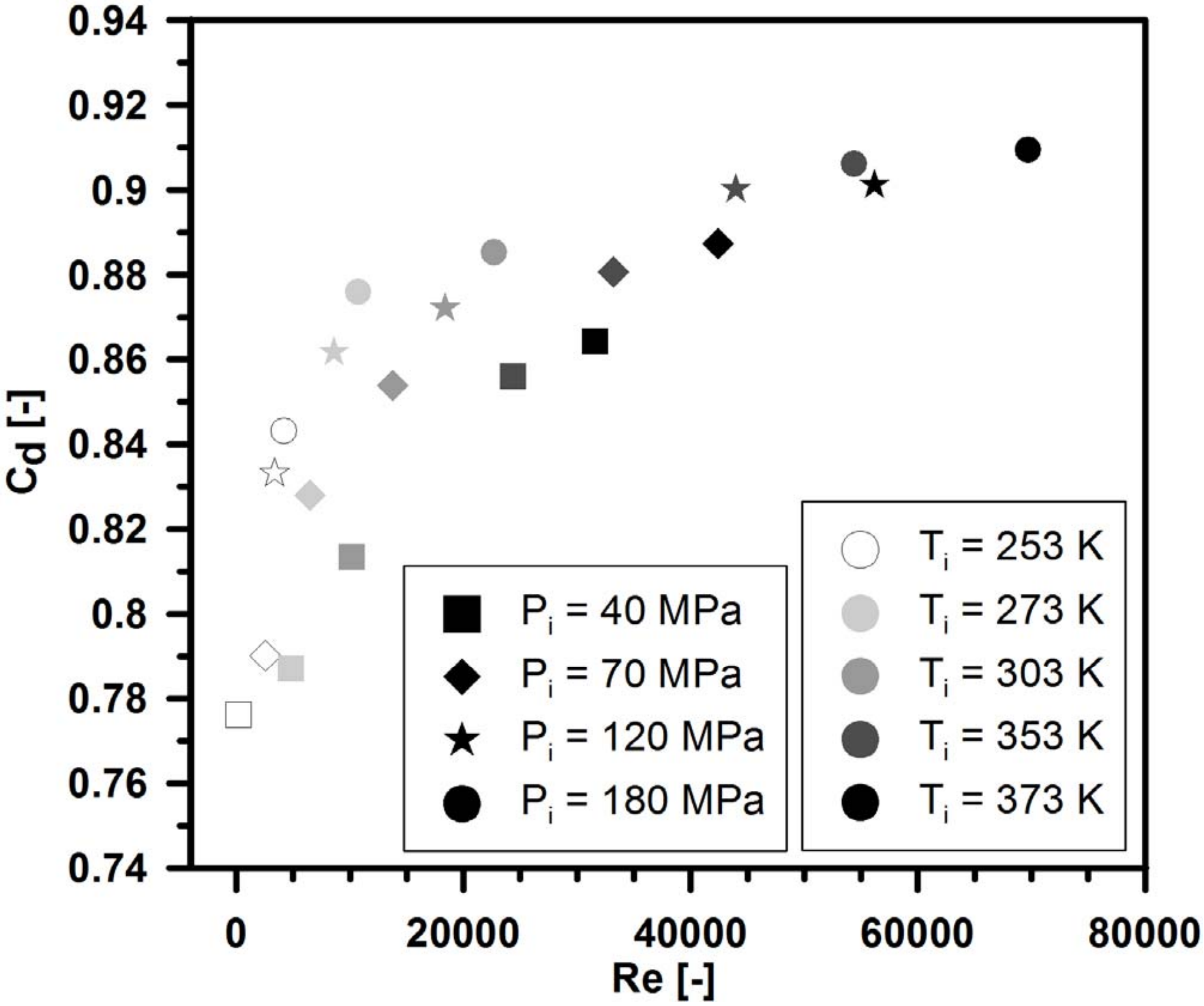

Figure 8: Injector discharge coefficient evolution against *Re* for the different tested conditions.

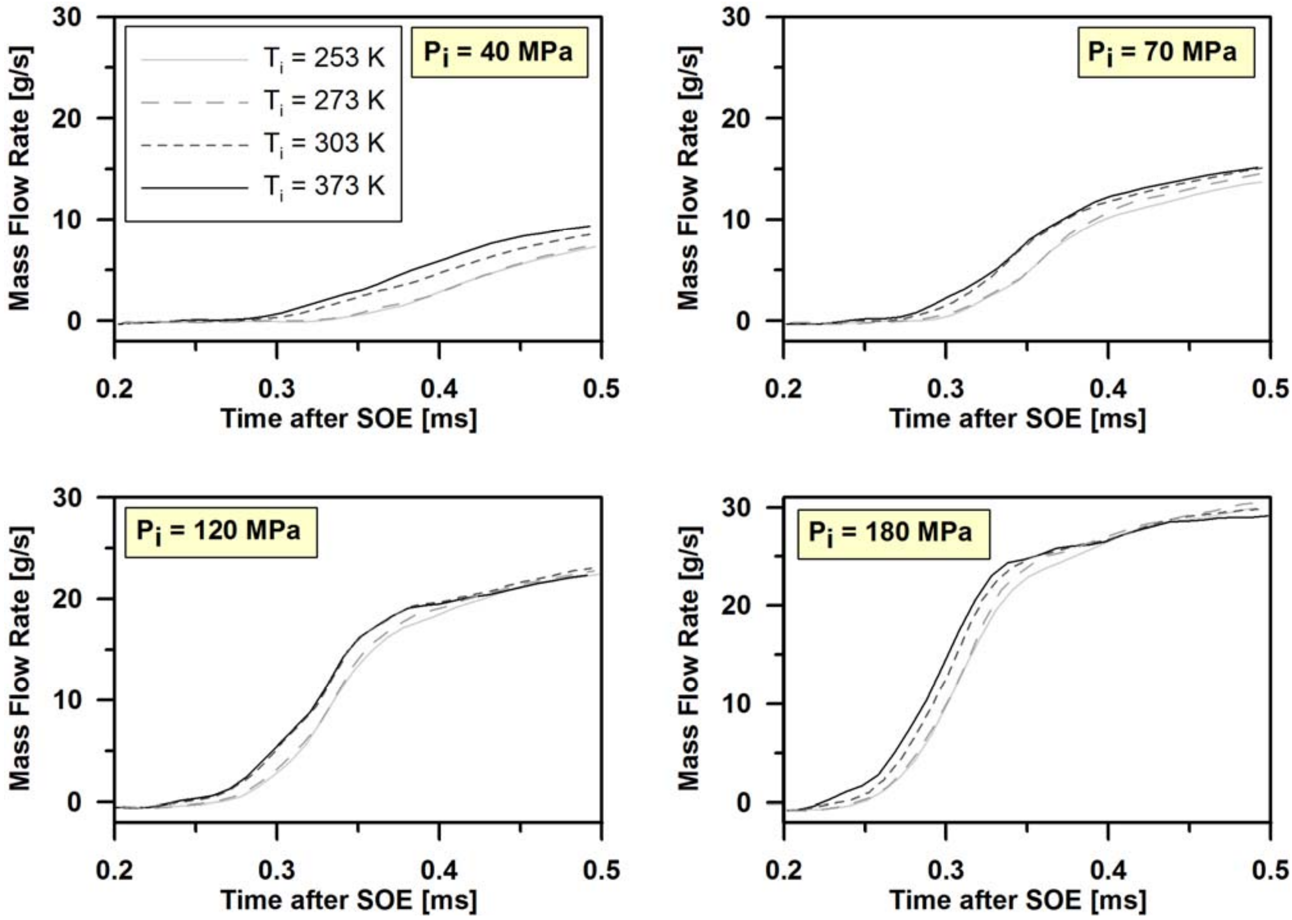

Figure 9: Detail of mass flow rate curves to highlight the injector behaviour on the opening stage.

Salvador, F.J., Gimeno, J., Carreres, M., Crialesi-Esposito, M., "Fuel temperature influence on the performance of a last generation common-rail diesel ballistic injector. Part I: Experimental mass flow rate measurements and discussion".

Energy Conversion and Management 114 (2016), pp. 364-375 (author version)

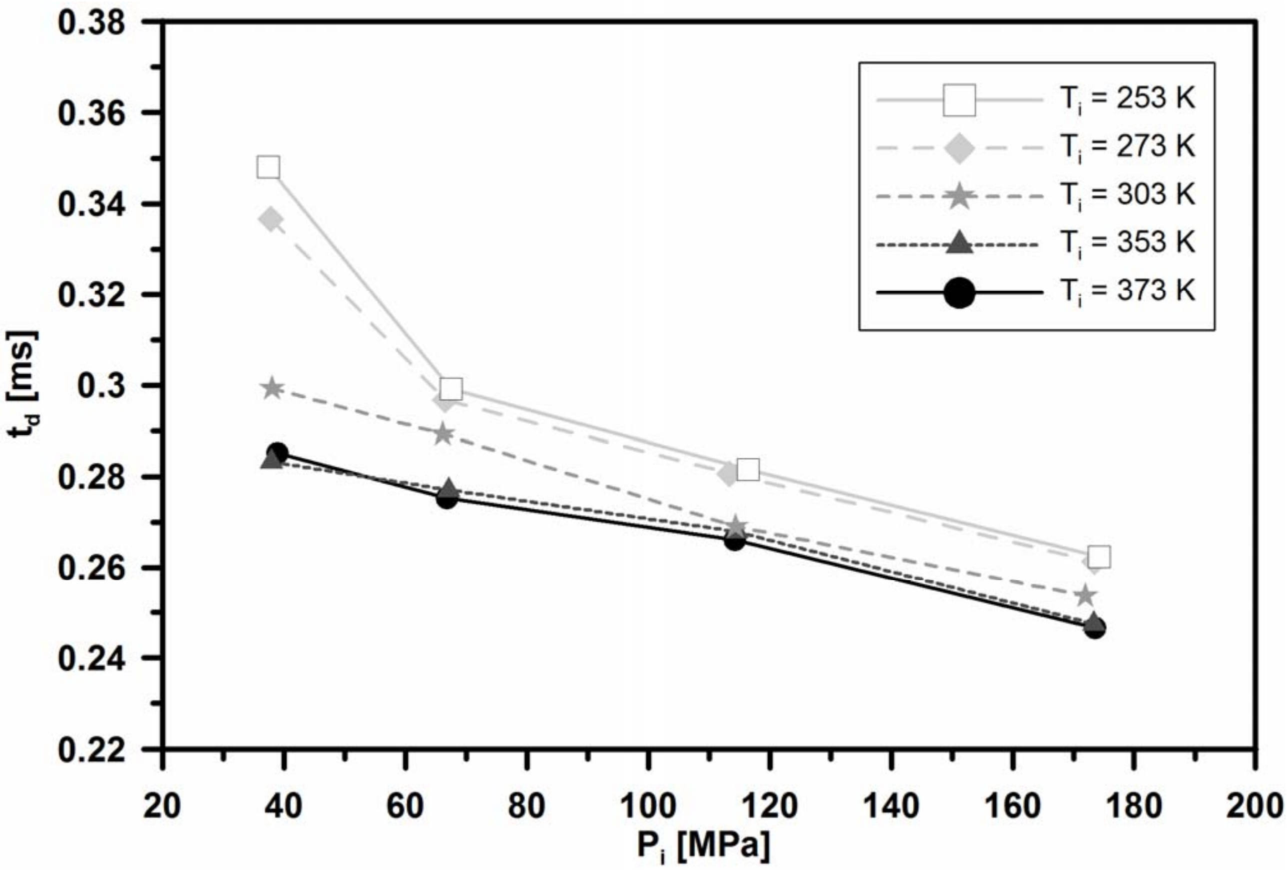

Figure 10: Evolution of the injection delay with the injection pressure for the different temperatures tested.

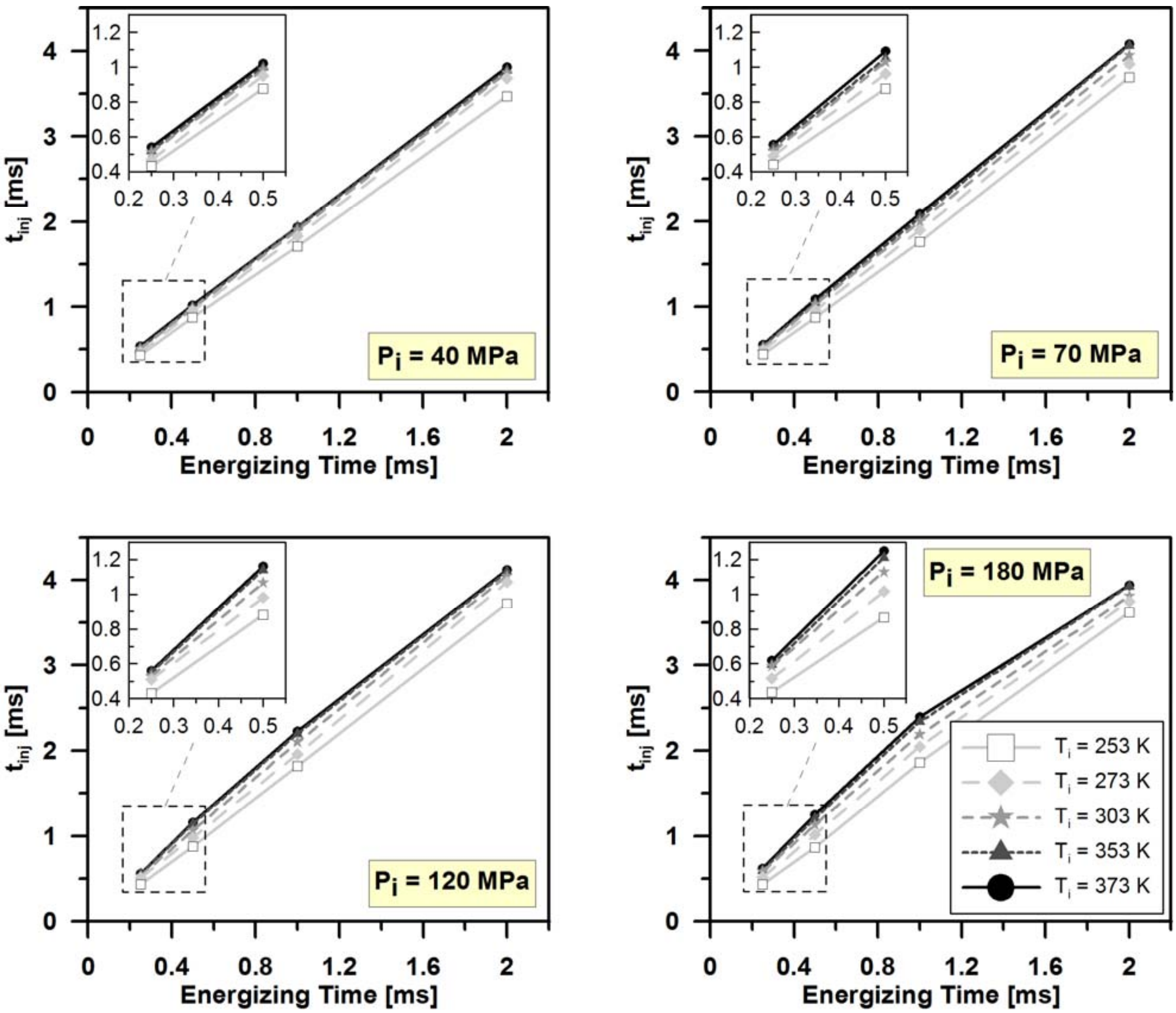

Figure 11: Injection time for all the tested conditions

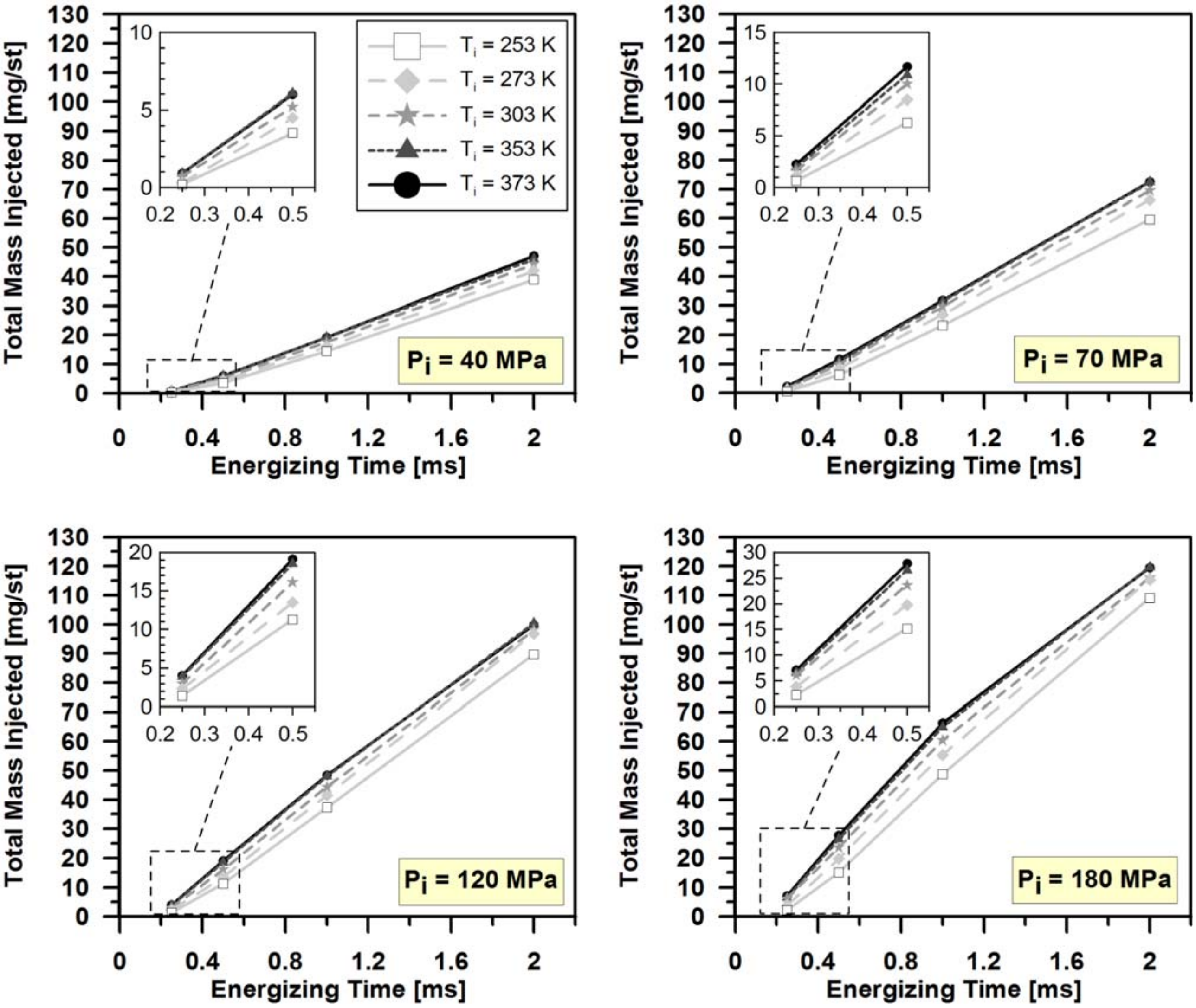

Figure 12: Total mass injected for all the tested conditions.

Salvador, F.J., Gimeno, J., Carreres, M., Crialesi-Esposito, M., "Fuel temperature influence on the performance of a last generation common-rail diesel ballistic injector. Part I: Experimental mass flow rate measurements and discussion".

Energy Conversion and Management 114 (2016), pp. 364-375 (author version)